HAL
open science

Non-Ohmic hopping transport in a-YSi: from isotropic to directed percolation

F Ladieu

To cite this version:

F Ladieu. Non-Ohmic hopping transport in a-YSi: from isotropic to directed percolation. Physical Review B: Condensed Matter and Materials Physics (1998-2015), 2000, 61, pp.8108 - 8118. 10.1103/PhysRevB.61.8108 . cea-01395493

HAL Id: cea-01395493

https://cea.hal.science/cea-01395493v1

Submitted on 10 Nov 2016

HAL is a multi-disciplinary open access archive for the deposit and dissemination of scientific research documents, whether they are published or not. The documents may come from teaching and research institutions in France or abroad, or from public or private research centers.

L'archive ouverte pluridisciplinaire **HAL**, est destinée au dépôt et à la diffusion de documents scientifiques de niveau recherche, publiés ou non, émanant des établissements d'enseignement et de recherche français ou étrangers, des laboratoires publics ou privés.

arXiv:cond-mat/9911433v1 [cond-mat.dis-nn] 26 Nov 1999

Non-Ohmic hopping transport in a-YSi: from isotropic to directed percolation

F. Ladieu*
Laboratoire Pierre Süe, DRECAM, CEA-Saclay, 91191 Gif / Yvette CEDEX, FRANCE
D. L'Hôte† and R. Tourbot
Service de Physique de l'Etat Condensé, DRECAM, CEA-Saclay, 91191 Gif / Yvette CEDEX, FRANCE

(Received

PACS numbers: 05.60+w - 64.60.Ak - 72.15.Rn - 72.20.Ht

Electrical transport has been investigated in amorphous $Y_{0.19}Si_{0.81}$, from 30 mK to room temperature. Below 2 K, the conductance G exhibits Efros-Shklovskii behavior $G \sim \exp[-(T_0/T)^{1/2}]$ at zero electric field, where conduction is expected to occur along a very sinuous path (isotropic percolation). The non-linear *I-V* characteristics are systematically studied up to very high fields, for which the conductance no longer depends on T and for which the current paths are expected to be almost straight (directed percolation). We show that the contributions of electronic and sample heating to those non-linearities are negligible. Then, we show that the conductance dependence as a function of low electric fields ($F/T < 5000\,\mathrm{V\ m^{-1}\ K^{-1}}$) is given by $G(F,T) = G(0,T) \times \exp(-eFL/k_BT)$. The order of magnitude (5-10 nm) and the T dependence ($\sim T^{-1/2}$) of L agrees with theoretical predictions. From the T_0 value and the length characterizing the intermediate field regime, we extract an estimate of the dielectric constant of our system. The very high electric field data do not agree with the prediction $I(F) \sim \exp[-(F_0/F)^{\gamma'}]$ with $\gamma' = 1/2$: we find a F dependence of γ' which could be partly due to tunneling across the mobility edge. In the intermediate electric field domain, we claim that our data evidence both the enhancement of the hopping probability with the field *and the influence of the straightening of the paths*. The latter effect is due to the gradual transition from isotropic to directed percolation and depends essentially on the statistical properties of the "returns" i.e. of the segments of the paths where the current flows *against* the electrical force. The critical exponent of this returns contribution which, up to now was unknown both theoretically and experimentally, is found to be $\beta = 1.15 \pm 0.10$. An estimation of the returns length is also given.

I. INTRODUCTION

The electrical transport in disordered insulators such as doped semiconductors or amorphous systems, has been widely investigated for several decades as a convenient way to probe the properties of Anderson insulators [1]. At finite temperature T, the conduction results a priori from all the electronic hops between any localized states i and j separated by a distance r_{ij} and a difference in energy E_{ij}. Starting from the probability of such a hop $p_{ij} \propto \exp -(r_{ij}/\xi + E_{ij}/k_BT)$ (with ξ the localization length and k_B the Boltzmann constant), Mott [2] introduced the key concept of variable-range hopping (VRH) stating that transport is dominated by *the most probable hops* whose characteristic length $r_m \propto T^{-1/(d+1)}$ and energy $E_m \propto T^{d/(d+1)}$ depend on T. As a result, the conductance G is predicted to follow

$$G = G_0 \exp\Big[-\Big(\frac{T_0}{T}\Big)^{\gamma}\Big] \tag{1}$$

where G_0 and T_0 are material dependent constants, and $\gamma = 1/(d+1)$ depends on the dimensionality d of the sample. Later, the percolation theory has been used to derive more rigorously Eq. (1) [3] [4]. In addition Efros and Shklovskii [5] found that electron interactions result in a "soft" Coulomb gap at the Fermi level, leading to $\gamma = 1/2$. It is currently admitted now [6] that Mott and Efros-Shklovskii laws are limiting cases of VRH. Both of them were observed experimentally as their relevance depends on the relative magnitudes of the hopping energy and Coulomb gap.

A. Electric field effects in hopping transport

The case of very high fields F, $eF\xi/(k_BT) \gg 1$ (e = electron charge) was studied through different theoretical approaches [7]-[12] which all predict that the current I should no longer depend on the temperature (activationless hopping) and behaves according to

$$I = I_0 \exp\Big[-\Big(\frac{F_0}{F}\Big)^{\gamma\prime}\Big] \tag{2}$$

where I_0 and F_0 are constants and $\gamma\prime = \gamma$ (see Eq. (1)). In spite of their similarity, Eqs. (1) and (2) correspond to completely different current path topologies. Eq. (2) is obtained by considering the shortest hops along which the electrostatic energy gain overcomes the energy fluctuations due to disorder [13], [7]. Thus in the very high field case, the hops occur in the direction of the field (*directed* percolation). On the contrary, for $F \to 0$, the current flows through a network of random impedances along *very sinuous* paths whose returns and meanders are such that any hop more resistive than the VRH prediction is forbidden. A quantitative description of these paths can be obtained by using the *isotropic* percolation theory [14] [15].

The intermediate field case $eF\xi/(k_BT) < 1$, where neither T nor F can be neglected is the most difficult one to handle theoretically, and the various models lead to different predictions that we summarize in the general equation giving the current

$$I(F,T) = I_1 \exp\Big\{-\Big(\frac{T_0}{T}\Big)^{\gamma}\Big[1 - A\frac{(eF\xi)^{\alpha}}{(k_BT)^{\alpha\prime}} + B\Big(\frac{eF\xi}{k_BT}\Big)^{\beta}\Big]\Big\} \tag{3}$$

where A, B, α, $\alpha\prime$ and β are parameters, A and B being positive. The first term $A(eF\xi)^{\alpha}/(k_BT)^{\alpha'}$ expresses the enhancement of the hopping probability when F grows. Depending on the authors, α and $\alpha\prime$ range from $\alpha = \alpha' = 1/(\nu+1)$ [10] (where $\nu \simeq 0.88$ for $d = 3$ is the critical index of the correlation radius) to $\alpha = \alpha' = 1$ [9], [13], and even $\alpha = 2$ and $\alpha' = 9/4$ for $d = 3$ [8], [12]. The discrepancies between these results come from the fact that the net current I_{ij} between two sites may increase exponentially with F or be insensitive to F, depending on the relative positions of the site energies. The second term $B(eF\xi/(k_BT))^{\beta}$ was predicted *only* by Böttger, Bryksin *et al.* [16]-[18] who addressed the additional problem of the "returns" , i.e. of the segments of the paths where the current flows *against* the electrical force. Their model states that the length of these returns decreases *gradually* when F increases. We show in this paper that our data evidence the existence of both terms of Eq. (3) with $\alpha = \alpha' = 1$ and $\beta = 1.15 \pm 0.10$.

B. Theories of hopping transport at intermediate fields

We recall here some theoretical points which are important for the interpretation of our data. The very sinuous current paths at $F \to 0$ can be pictured by using the "nodes-links-blobs" concept [14] [15], derived from the isotropic percolation theory : at small scales the current path consists of a fractal-like network of connected conductances up to the "blob" scale $\mathcal{L}_p$, and the blobs are the links of a homogeneous network. In the linear regime, the conductances inside a blob are much larger than the key conductances $G_{key} \sim \exp-(T_0/T)^\gamma$ lying at the end of each blob. G_{key} sets the overall sample conductivity since at scales larger than $\mathcal{L}_p$ the system is homogeneous. For the intermediate field case, where neither T nor F can be neglected, three main effects have to be considered :

(i) for a site i belonging to the percolation path, the density of sites j yielding a non negligible conductance G_{ij} is modified by F;

(ii) a field-induced rearrangement of the charge along the current paths can take place : the local chemical potential μ_i can fluctuate widely around the mean value given by eFr_i;

(iii) the lengths of the "returns", i.e. the segments where the current has to go against the electrical force, decrease when F increases.

Most authors disregarded (iii) and focused upon (i) and (ii), yielding predictions summarized by Eq. (3) with $B \equiv 0$. However, they gave diverging predictions depending on the relative influence given to (i) and (ii). For example, Pollak and Riess [9] find $\alpha = \alpha' = 1$ and $A = 3/32$ in a model where (i) plays the central role, and the correlations between nearest neighbors conductances are taken into account. They find that (ii) is quite negligible ($\delta\mu_i \leq k_BT$). This contradicts Shklovskii model [10] ($A \simeq 1$ and $\alpha = \alpha' = 1/(1+\nu) \simeq 0.53$ for $d = 3$) which emphasizes (ii) ($\delta\mu_i \gg k_BT$) by concentrating almost *all* the electrical potential drops existing at the blob scale $\mathcal{L}_p$ upon the key conductance. The disagreement between these predictions was never completely explained [19] even if numerical simulations by Levin and Shklovskii [20] suggested that the Pollak and Riess result holds in usual experimental conditions $(T_0/T)^{1/(d+1)} \leq 70$ while Shklovskii result would hold in the opposite case, i.e. at exceedingly low temperatures. Two other groups found different results : Apsley *et al.* [8] and Van der Meer [12] obtained $\alpha = 2$, $\alpha\prime = 9/4$, but their methods were criticized since the former did not take into account the directed percolation requirement, while the latter uses dimensional "invariants" which were shown later to be F dependent [21].

Taking (iii) into account[16][21][22] prevents the current from increasing too fast : the corresponding second term $B(eF\xi/k_BT)^\beta$ in Eq. (3) reduces the exponential increase of I due to $-A(eF\xi)^\alpha/(k_BT)^{\alpha\prime}$. The physical reason is that the returns act as "bottlenecks" for the current. The problem being exceedingly complicated, the precise values of α, β, A, B were found to depend on the various methods used by Böttger, Bryksin *et al.* The last and more accurate results were obtained numerically [22][17] [18] : $\alpha = \alpha\prime = 1$, $A = 1/6$, $B \simeq 0.02$, $1/\beta \simeq 1.1$ (this latter parameter is the critical exponent of the returns length Λ, see below Eq. (12)). The theoretical value of β *is given within an error of* 50% *due to numerical uncertainties.* Yet, the *precise* value of β is of major importance since for $\beta < \alpha$, the differential conductivity $\sigma = \partial I/\partial V$ decreases at low fields to reach an absolute minimum at a finite F. On the contrary, in the case $\beta > \alpha$, σ increases at low fields and has no absolute minimum at finite field.

The above mentioned theories disregard the possible F-dependence of the carrier density due to trapping in dead ends of paths, as well as the possible F-dependence of the localization length ξ. Fortunately, both effects should be negligible in our case. Indeed, *statistically* as many holes as electrons become trapped when F increases, as in our case the density of states is symmetric around the Fermi level (parabolic Coulomb gap)[23]. The $\xi(F)$ dependence should be negligible [24] as long as $E_F \gg eF\xi$ where E_F is the kinetic energy at the Fermi level: this is the case in our sample[25].

C. The experimental situation

On the experimental side, I-V non linearities were investigated both in amorphous materials [26]-[34] and in doped crystalline semiconductors [35]-[47]. In most of these works, the authors focussed either on very high fields or on intermediate fields. For intermediate fields, the data [28] [29] [31] [35]-[42] [45] were analyzed using the electric field dependence predicted by Hill [13], Pollak and Riess [9], and Shklovskii [10]

$$\ln\big(G(F,T)\big) = \ln\big(G(0,T)\big) + \frac{eFL}{k_BT} = \ln\left(G_0\right) - \left(\frac{T_0}{T}\right)^\gamma + \frac{eFL}{k_BT} \qquad (4)$$

where L is a length related to the hopping distance $r_m = (\xi/2)(T_0/T)^\gamma$. Hill[13] and Pollak and Riess[9] predict $L = C.(\xi/2)(T_0/T)^\gamma$ with $C = 0.75$ or 0.18, while Shklovskii predicts $L \propto T^{-(1+\nu)\gamma}$ [10] with $\nu = 0.88$. Eq. (4) results from Eq. (3) by neglecting the returns term ($B = 0$) and by assuming that the F and T dependences of G and I are close to each other. The experimental values of L and their T dependence often disagree with the theoretical predictions [31] [36]-[38][40]. The claim by Wang *et al.* [44] that the non-linearities in Ge:Ga were due to carriers heating [64] rather than to the preferential hopping along the electric field which leads to Eqs. (3) or (4) triggered hot-electron analyses of the data [47]-[53]. They show that the relative contribution of carriers heating and electric field effects has to be considered at very low temperature. In very high electric fields, the expected activationless conduction (see Eq. (2)) has been observed by several authors [30]-[32] [42] [43] [46]. The equality of the VRH and activationless exponents (γ and $\gamma\prime$ in Eqs. (1) and (2)) has been checked for $\gamma = 1/2$ in several systems [32] [43], but $\gamma\prime = 1/4$ and $\gamma = 1/2$ has been found in amorphous GeCu[31].

In this work we systematically investigate the whole set of non linearities ranging from the linear VRH regime at $F \to 0$, to the activationless conduction at very high fields : in our low temperature domain (0.03 K $\leq T \leq$ 1.3 K), F/T varies from 1.5×10^2 $\mathrm{V\,m^{-1}\,K^{-1}}$ to 1.4×10^6 $\mathrm{V\,m^{-1}\,K^{-1}}$. Our samples are made of amorphous $Y_{0.19}Si_{0.81}$. In comparison to most of the experimental works performed in this low temperature range ($<$ 1 K) [37] [43]-[47], we go to higher values of F and F/T, thus allowing an investigation of both the intermediate and the very high field regimes. At very low temperatures, this has been done by Rosenbaum *et al.* on Si:P [37], however the authors found an abnormally large value of L. At higher temperatures, these two regimes were investigated for *a*-GeCu at 1.6 K $< T <$ 110 K [31] and ZnSe at 1.6 K $< T <$ 4.2 K [42]. The first paper raised the question of unexpected exponents values (in the L vs. T and $\ln(G)$ vs. F dependences) while the second one found a puzzling decrease of L when F increases. Clearly, new data are needed. In this work, we test the validity of Eqs. (1)-(4) and show that they are in good agreement with our data for intermediate fields. In particular we find $L \simeq C.r_m$ [13][9]. We also check that the contribution of heating effects to the non-linearities is negligible. Our main result is that Eq. (3) with $\alpha = \alpha\prime$ is more suitable than Eq. (4) to fit the data : this allows us to estimate the size of the returns and the value of the related critical exponent β[16]-[18]. Finally, we show that in the activationless region, the I vs F dependence is more intricate than the law given by Eq. (2).

The paper is organized as follows. In section II we describe the experimental setup and method. The conductance as a function of the temperature in the region $F \to 0$ is presented in section III. In section IV, we consider the very high field case. Having extracted the physics of the two extreme F regimes, we finally turn in section V to the intermediate field case. Finally, we summarize our main results in section VI. In appendix A we show that heating mechanisms cannot explain the $I - V$ non-linearities, while appendix B is devoted to the extraction of the localization length from the data.

II. EXPERIMENT

As shown in Fig. 1, each amorphous Y_xSi_{1-x} sample studied ($x \simeq 0.19$) is deposited on a sapphire substrate on which two interdigited gold electrodes were evaporated and etched. The spacing between the electrodes is $l = 128\,\mu$m. The Y_xSi_{1-x} layers were obtained by Argon plasma sputtering on the sapphire substrate (cooled at 77 K to prevent Y or Si aggregates formation), using a Y_xSi_{1-x} source. The thickness of the layers is $9\,\mu$m, much larger than any hopping length, hence electrical transport is three dimensional. Previous studies of electrical transport in such Y_xSi_{1-x} samples [54]-[59], have shown that a small variation of x allows to cross the metal-insulator transition : above $x \simeq 0.22$ the samples are metallic; while for lower values of x, the samples exhibit an insulating behavior, i.e. a divergence of the resistance for $T \to 0$, in agreement with the VRH predictions [55]-[58], except for the very weakly insulating samples at the lowest temperatures [59]. In the present work $x \simeq 0.19$ and the samples are strongly insulating, exhibiting VRH below $T \simeq 2$ K. Since the two samples we used behaved similarly, we report only the data of one of them.

As shown in Fig. 1, a great attention was paid to the thermalization of the sample because of a possible heating interpretation of the *I-V* curves non-linearities. As explained in Appendix A, we measured the thermal conductances involved in our sample and concluded that heating effects were irrelevant in our sample: neither heating of the whole sample nor carrier heating can explain the *I-V* non linearities reported here.

Electrical contacts were made by ultrasonic soldering of two gold wires on the evaporated electrodes. The data were obtained by setting a given voltage $V = Fl$ on the sample, and by waiting for a time τ before measuring the current I. We paid the greatest attention to choosing τ large enough to let the current settle, e.g. we took $\tau(T < 800\,\mathrm{mK}) \geq 100\,\mathrm{s}$. The temperature was registered for each $I(V)$ point, and its stability proved to be better than 1%. The coaxial cables used were previously tested alone (in an open circuit, at all temperatures) to check that their leakage current was negligible. Let us note that it is unlikely that the gold-YSi electrical contact resistance plays a role since the contact area is very large and in previous similar works [58], it was shown to play no role. The fact that the temperature dependence $G(0,T)$ we observe follows a VRH law (see next section) is an additional indication that the contact resistance is negligible. Finally, the symmetry of the *I-V* curves with respect to current and voltage reversing was checked.

III. BEHAVIOR AT $F \to 0$

The *I-V* characteristics are shown in Fig. 2 where, for clarity, we report only the curves for 18 different temperatures out of the 36 ones we measured. As shown in the inset, the resistance (R) - temperature law is simply activated from room temperature to $\simeq 10\,\mathrm{K}$: we find $R = R_1 \exp(-T_1/T)$ with $T_1 = 40 \pm 4\,\mathrm{K}$ and $R_1 \simeq 88 \pm 2\,\Omega$. For $T < 8\,\mathrm{K}$ the divergence of the resistance when $T \to 0$ becomes *weaker* (see inset of Fig. 2), which is a standard indication that VRH takes place at low temperature [5]. Let us note that simple activation for $T \geq 10\,\mathrm{K}$ is usually interpreted as due to thermal excitation from the Fermi level E_F to the mobility edge E_{Mob} where electronic states are delocalized; thus $k_B T_1 = E_{Mob} - E_F$.

To study the temperature dependence of the conductance at $F \to 0$, we plotted our data in the (F/T, $\ln(V/I)$) plane (see Fig. 3). The $G(F \to 0)$ values were obtained from an extrapolation of the curves towards low fields. To allow for a precise extrapolation, this procedure was restricted to the $0.4\,\mathrm{K} < T < 1.3\,\mathrm{K}$ cases. The extrapolated values were obtained from a linear fit of the first points in each curve (lower F/T values). We checked that those values did not depend significantly on the number of points selected in the fit. The expected VRH temperature-conductance law is given by Eq. (1) where $\gamma = 1/2$ or $\gamma = 1/4$. Discriminating between these exponents is hardly achieved by looking for a straight line in the $\ln(G(F \to 0))$ versus $T^{-\gamma}$ plot, as the lines always *seem* straight. The comparison between the different exponents γ is improved by plotting a normalized value of $T^{-\gamma}$, i.e. $(T^{-\gamma} - T_{Min}^{-\gamma})/(T_{Max}^{-\gamma} - T_{Min}^{-\gamma})$ where T_{Min} and T_{Max} are the two extreme values of T selected for the plot. In Fig. 4, we see that $\gamma = 1/2$ is favored in comparison with $\gamma = 1/4$. A fit of $\ln(R(F \to 0))$ vs. T using Eq. (1) in which G_0 and T_0 are free parameters yields a residue (measured minus fitted value) shown in the inset of Fig. 4 : clearly, there is a correlation between the residue and T only for $\gamma = 1/4$. The normalized χ^2 per point is 1.1 for $\gamma = 1/2$, and 9.0 for $\gamma = 1/4$. If γ is a parameter of the fit, we find $\gamma = 0.47 \pm .02$. We thus conclude that $\gamma = 1/2$, and using this value in the fit, we get $T_0 = 257 \pm 1.5\,\mathrm{K}$ and $R_0 = 1/G_0 = 92 \pm 5\,\Omega$. Following Efros and Shklovskii,

$$k_B T_0 = \frac{2.9 e^2}{4\pi\epsilon_0\epsilon_r\xi} \tag{5}$$

where $\epsilon_0\epsilon_r$ is the dielectric constant of the system. We shall see in Appendix B that the non-linearities analysis together with Eq. (5) allow to extract an information on ξ and ϵ_r separately.

IV. RESULTS AT VERY HIGH FIELDS

In the very high fields case, $eF\xi/(k_B T) \gg 1$, the theory [7] states that the current results from hops between sites i and j, such that $E_{ij} = eFr_{ij}$. For these activationless hops, $I_{ij} \propto \exp(-2r_{ij}/\xi)$, which, using a maximization procedure leads to Eq. (2) with[7]

$$F_0 = N_2 \frac{k_B T_0}{e\xi} \tag{6}$$

where N_2 is a numerical constant which can be calculated within the directed percolation theory. For Mott's VRH ($\gamma = 1/4$) Pollak and Riess obtain $N_2 = 4.8$. For the Efros-Shlovskii VRH ($\gamma = 1/2$), N_2 has not been calculated to our knowledge.

Our lowest temperature data should belong to the very high field domain, as the two I-V curves corresponding to $T = 29\,\mathrm{mK}$ and $T = 49\,\mathrm{mK}$ are identical. Indeed, we shall see that the low and intermediate field data analysis lead to $\xi \approx 7\,\mathrm{nm}$ (see Appendix B), hence $eF\xi/(k_BT) \geq 50$ for $T = 29\,\mathrm{mK}$. The 29 mK data can be rather well fitted by using Eq. (2) with $\gamma\prime = 1/2$, I_0 and F_0 being free parameters. It yields $F_0 = (3.8 \pm .05) \times 10^7\,\mathrm{V/m}$, hence $4 \leq N_2 \leq 11$ by using the upper and lower values of ξ. The normalized χ^2 per point is however 290. Thus, in spite of the reasonable extracted F_0 and N_2 values, the relevance of the fit must be questioned. Indeed, if we fit the whole $I(F, 29\,\mathrm{mK})$ data using Eq. (2), $\gamma\prime$ being a free parameter, we get $\gamma\prime = 0.65 \pm 0.01$ and a χ^2 per point of 94.

To investigate the problem, we give in Fig. 5 the F dependence of the effective exponent γ_{eff} defined by

$$\gamma_{eff} = -\frac{\partial \ln\left(\frac{\partial \ln I}{\partial \ln F}\right)}{\partial \ln F}. \tag{7}$$

If $I(F)$ is given by Eq. (2), then $\gamma_{eff} = \gamma\prime$. For $T > 200\,mK$, γ_{eff} is always negative, while for $T < 200\,\mathrm{mK}$, γ_{eff} it is negative for the lower F values. This can be related to the fact that in the intermediate field region, the $I(F)$ dependence should obey Eq. (3) for which the expected γ_{eff} is F-dependent. For the lowest temperatures, γ_{eff} becomes positive when F increases, but there is no saturation at $\gamma_{eff} = 0.5$. Instead, a maximum is reached at a value between 0.5 and 1, even if a convergence of γ_{eff} towards 1/2 might exist at fields larger than $4 \times 10^4\,\mathrm{V/m}$.

We suggest that these values of γ_{eff} between 0.5 and 1 are due to the fact that the very high field conduction results from an interplay between activationless hopping (for which $\gamma_{eff} = 1/2$) and *tunneling across the mobility edge*. Indeed, the latter process leads to the simple activated law [33], [60]

$$I \sim \exp\left[-(\frac{4}{3eF})\sqrt{\frac{2m(k_BT_1)^3}{\hbar^2}}\right] = \exp\left[-\frac{F_1}{F}\right] \tag{8}$$

where k_BT_1 is the energy difference between the Fermi level and the mobility edge. Since $T_1 \simeq 40\,\mathrm{K}$ (see Sec. III), $F_1 = 1.4 \times 10^6\,\mathrm{V/m}$. The fit of the $I(F, 29\,\mathrm{mK})$ data for the interval $F > 2.8 \times 10^4\,\mathrm{V/m}$ where $\gamma_{eff} > 0.5$, using $I = I_1 \exp(-F_1/F)$, yields a normalized χ^2 per point of 40 and $F_1 = (5.5 \pm 0.05)\,10^5\,\mathrm{V/m}$, which is only a factor 2.5 below the calculated value. We cannot interpret the $\gamma_{eff}(F)$ curves more precisely since, to our knowledge, there exists no theory taking into account both the disorder in the localized band states and the tunneling through the Mobility Edge.

It is interesting to note that if activationless hopping was the only transport mechanism in the very high field regime, the critical value $(F/T)_c$ at which the transition from Eq. (3) to Eq. (2) occurs would be temperature independent : this can be readily seen by equating the rhs of Eqs. (2) and (3) at $F/T = (F/T)_c$ and disregarding pre-exponential factors. If we define, for any given T the experimental critical field value F_c by $I(F_c, T) = k\,I(F_c, 29\text{ mK})$, with $k = 1.1$, we find that in our sample, $(F/T)_c$ is clearly T-dependent: it increases by a factor 3.5 when the temperature decreases from 413 mK to 74 mK.

V. RESULTS AT INTERMEDIATE FIELDS

We can see on Fig. 3 that our experimental points line up in almost parallel curves in the ($\ln(R)$, F/T) plane. Clearly, they are not really straight lines, hence Eq. (4) does not hold with precision. However, in the spirit of the majority of previous works, we first use Eq.(4) and extract the length $L(T)$ defined by $\ln[G(F)/G(F \to 0)] = eFL(T)/(k_BT)$ for F just above the linear regime. We show in a second step that Eq. (3) is much more relevant to account for our data.

A. Extraction of $L(T)$ using Eq. (4)

The slopes of the $\ln(R)$ vs. F/T curves for $F \to 0$ were extracted for the different temperatures where it was possible, i.e. $0.4\,\mathrm{K} < T < 1.3\,\mathrm{K}$ (see Fig. 3). A linear fit yielded a normalized χ^2 per point close to 1 only for $F/T < 5000\,\mathrm{V\,m^{-1}\,K^{-1}}$. We restricted the L extraction to this interval where the curves are linear. The result is shown in Fig. 6. A fit of these points using the law $L = L_0\,(T_0/T)^\zeta$ where L_0 and ζ are free parameters gives $\zeta \simeq 0.65$ with a normalized χ^2 per point of 0.7. Constraining the fit with $\zeta = 0.5$ leads to $L_0 = (0.52 \pm 0.01)$ nm and a normalized χ^2 per point of 1.1 : the resulting curve is shown in

Fig. 6. As a consequence, we can state that the Shklovskii prediction [10] $\zeta = 2\gamma = 1$ does not hold for our system, while the predictions of Hill [13] and Pollak and Riess[9], $L \propto r_m$ leading to $\zeta = \gamma = 1/2$, are in agreement with our results. It is interesting to note that the values of $L(T)$ remain roughly the same if they are extracted from linear fits of the *whole* $\ln(R)$ vs. F/T curves, although these fits yield a normalized χ^2 per point varying between 3 and 250. The localization length ξ extracted from $L_0 = C.(\xi/2)$ with the Pollak and Riess value $C = 0.17$ [9] yields $\xi \simeq 6\,\mathrm{nm}$. We shall come to this point more in detail later.

B. Extraction of the parameters of Eq. (3)

We turn to the main result of our study, namely the relevance of the Böttger *et al.* prediction [17] concerning the "returns" and summarized in Eq. (3).

B.1. F/T is the *unique* relevant parameter

We define, so as to test Eq. (3),

$$\Psi(F,T) = \sqrt{\frac{T}{T_0}} \ln\left(\frac{I(F,T)}{I_{E.S.}(F,T)}\right) \text{ , with } I_{E.S.}(F,T) = \frac{V}{R_0} \exp\left[-(\frac{T_0}{T})^{1/2}\right] \quad (9)$$

where $V = Fl$, $R_0 = 92\,\Omega$ and $T_0 = 257\,K$ (see Sec. III). It is easy to show that if Eq. (3) holds in what concerns the $G(T,F)$ dependence (instead of $I(T,F)$), Ψ is just equal to $A(eF\xi)^{\alpha}/(k_BT)^{\alpha'} - B(eF\xi/k_BT)^{\beta}$. We have chosen to perform our analysis on $G(T,F) = I(T,F)/(Fl)$ rather than on $I(T,F)$ because all the above depicted theories do not allow to recover a linear regime when $F \to 0$: in this case, Eq. (3) gives $I(F \to 0) = I_1 \exp\left[-(T_0/T)^{\gamma}\right]$ which is not consistent with Eq. (1). Note that this difficulty has been ignored in almost all experimental works dealing with the intermediate fields case, as they focus upon $G(F)$ rather than on $I(F)$. Numerically, our choice is justified by the fact that the exponential $I(F)$ dependence in Eq. (3) is much faster than the contribution of the denominator of $G(F) \sim I(F)/F$ (see also [61]).

To perform our analysis of the intermediate field case, we suppressed the data points corresponding to the very high field case (see Sec. IV). This was done by selecting 7164 $I(F,T)$ points among the whole set of 8189 points, on the criterion $I(F,T)/I_{VHF}(F) - 1 \geq 10\%$, where $I_{VHF}(F)$ is the very high field current defined by $I_{VHF}(F) = I(F, T = 29\,mK)$. The 10% criterion is rather arbitrary, but we checked that our results do not depend on its precise value, provided it remains above 5%. Then, Ψ is calculated for each of these 7164 points. As shown on Fig. 7, $\Psi(F,T)$ *is a universal function of* F/T over more than 3 orders of magnitude, while the 7164 experimental points correspond to 36 different temperatures ranging from 49 mK to 1.29 K.

The fact that $\Psi(F,T)$ depends only on F/T implies $\alpha = \alpha'$, which definitely shows that both Apsley [8] and Van der Meer [12] models are not relevant for our sample. Moreover, the log-log slope of $\Psi(F/T)$ *at the lowest* F/T values is very close to 1 and clearly larger than $1/(\nu+1) \simeq 0.53$ which means that Shklovskii prediction [10] does not hold. This is not surprising since in our experiment $(T_0/T)^{1/2} \leq 70$ which is a domain where the numerical work of Levin and Shklovskii [20] leads to $\alpha = 1$. However our data are poorly fitted by the Hill [13] and the Pollak and Riess[9] prediction $\Psi \sim F/T$ since the log-log slope of $\Psi(F/T)$ decreases as F/T increases. More generally, a fit of $\Psi(F/T)$ with a unique power law $(F/T)^{\alpha''}$ gives a poor agreement whatever α'', especially because of the points in the region $F/T \geq 3 \times 10^4\,\mathrm{V\ K^{-1} m^{-1}}$. The only remaining prediction is thus the one of Böttger *et al.* where $\alpha = 1$ and β is unknown theoretically. In the next section this prediction will be *assumed* and the best value of β will be sought. Quite interestingly, the fit of Ψ we obtain in the next section is, by far, much better than all the "reasonably simple" fits we tried: for example attempting a polynomial fit with $\Sigma_{i=1}^{m} a_i (F/T)^i$ gives a poor agreement even if m is as large as 5.

B.2. Extraction of the critical exponent β assuming $\alpha = 1$.

We thus have to fit the $\Psi(F/T)$ points using the function

$$\Gamma\frac{F}{T} - \Delta(\frac{F}{T})^{\beta} \quad (10)$$

with Γ, Δ, β as free parameters. Since the $\Psi(F/T)$ values extends over several orders of magnitude, we perform the fit on $\ln(\Psi)$, i.e. we request that a *relative* error $\mathcal{E}$ per point is minimal, with $\mathcal{E}$ defined by

$$\mathcal{E}^2 = \frac{1}{7164 s^2} \sum_{j=1,7164} (1-x)\Big[\ln\Big(\frac{\Psi\big((F/T)_j\big)}{\Gamma(F/T)_j - \Delta(F/T)_j^{\beta}}\Big)\Big]^2$$

$$+x\Big[\ln\Big(\frac{\Gamma(F/T)_j - \Psi\big((F/T)_j\big)}{\Delta(F/T)_j^{\beta}}\Big)\Big]^2, \qquad (11)$$

where x is a weight to be chosen in the $(0,1)$ interval and $s^2 = \big\langle(\ln(\Psi) - <\ln(\Psi)>)^2\big\rangle \simeq (0.08)^2$ is the variance of $\ln(\Psi)$ drawn from the data. Note that the first term in the rhs of Eq. (11) is the relative error per point on Ψ while the second one is the relative error per point on the "Böttger second term" of Eq. (3), $\Delta(F/T)^{\beta}$. The minimization of those two terms has *opposite effects* on the optimal value of β. Indeed keeping only the first one (i.e. setting $x = 0$) leads to $\beta = 1.38 \pm 0.03$ and yields a good agreement between the $\Psi((F/T)_j)$ points and the fitted curve, but leads to a discrepancy between $\Gamma(F/T)_j - \Psi\big((F/T)_j\big)$ and $\Delta(F/T)_j^{\beta}$ which becomes clearly too large when $F/T < 5 \times 10^4$ V K^{-1} m^{-1}. Conversely, setting $x = 1$ leads to $\beta = 1.03 \pm 0.03$, with $\Gamma(F/T)_j - \Psi\big((F/T)_j\big) \simeq \Delta(F/T)_j^{\beta}$, but a discrepancy appears between the $\Psi\big((F/T)_j\big)$ points and the fitted curve, especially at high F/T values. Keeping x in the $(0.05, 0.95)$ interval leads to optimal values $\beta(x)$ in the $(1.05, 1.15)$ range, i.e. to an uncertainty on β not very much larger than the one obtained for a given x. We finally keep the larger error bar on β and find : $\beta = 1.15 \pm 0.1$, $\Gamma = (1.25 \pm 0.5) \times 10^{-5}$ K m/V and $\Delta = 1.4 \times 10^{-6}$(m K/V)$^{\beta}$ ($\Delta^{1/\beta}/\Gamma = 0.70 \pm 0.07$). The solid line on Figs. 7 and 8 is the fit resulting from $\big(\beta = 1.15; \Gamma = 1.25 \times 10^{-5}\mathrm{K\,m\,V^{-1}}; \Delta = 1.4 \times 10^{-6}(\mathrm{K\,m\,V^{-1}})^{\beta}\big)$: the agreement with the data is good ($\mathcal{E}(x = 0.5) = 0.72$) and the only systematic deviation occurs at the very few highest F/T values where the transition to the very high fields regime occurs.

The comparison of Eqs. (3) and (10) gives $\Gamma = Ae\xi/k_B$. From $\Gamma = 1.25 \times 10^{-5}$ m K/V we deduce $A\xi = 1.1$ nm. Unfortunately, the precise value of A is not known in our case of Efros Shklovskii's hopping ($\gamma = 1/2$). As shown in Appendix B, using $T_0 = 257$ K, $A\xi = 1.1$ nm as well as considerations about the dielectric constant ϵ_r we conclude that $\xi \approx 7$ nm. We cannot be more precise due to the various unknown numerical factors involved in the predictions we used, but we note that these values of ξ compare favorably to previous results obtained on Y_xSi_{1-x} samples much closer to the metal-insulator transition [58], [59] where larger values of ξ were found (a few tens of nm).

We compare now the analysis performed just above with the one carried out using Eq. (4) which yielded $L = L_0\,(T_0/T)^{1/2}$ with $L_0 = 0.52$ nm, and $\xi \simeq 6$ nm, using $L_0 = C\,(\xi/2)$ and $C = 0.18$ (see Sec. B.). Neglecting the weak difference between the $G(T,F)$ and the $I(T,F)$ dependences, the comparison of Eqs. (3) and (4) leads to $L_0 = A\xi$ if the additional term $B(eF\xi/(k_BT))^{\beta}$ in Eq. (3) is *assumed not to change* L_0. Clearly, we have a discrepancy by a factor 2 between L_0 and $A\xi = 1.1$ nm : this was checked to come from the $B(eF\xi/(k_BT))^{\beta}$ term in Eq. (3). Surprisingly both analysis yield roughly the same $\xi \approx 6 - 7$ nm for $A = 1/6$ and $C = 0.18$.

B.3. Extraction of the return length Λ.

We now turn to the analysis of the "returns" size. As explained above, β and Δ give an information about the typical length Λ of the returns which decreases gradually as F increases. Indeed, according to Böttger *et al.* [22], if $\rho = \ln[I(F,T)/I_1]$ (ρ is the argument of the exponential in Eq. (3)), Λ is given by

$$\Lambda(\rho) \simeq 2\delta r_m \Big(\frac{\rho_c}{\rho - \rho_c}\Big)^{\frac{1}{\beta}} \Big(\frac{\rho_m - \rho}{\rho_c}\Big)^{\mu} \qquad (12)$$

where $\mu = 1.0 \pm 0.3$ and $\delta \simeq 0.25$ are numerical constants [22], ρ_m is the directed percolation threshold, and $\rho_c = (T_0/T)^{\gamma}$. In the linear regime it is found that $\rho(F \to 0) \simeq \rho_c + 1$ [14], yielding a finite value of $\Lambda(F \to 0)$. Increasing F up to the intermediate field region leads to a ρ increase, thus to a Λ decrease. Increasing F further, ρ reaches ρ_m and Λ vanishes indicating that the current paths are directed. The maximum length Λ_{max} of the returns is thus obtained just at the onset of the non linear regime, where we

can put in Eq. (12) $\rho = (T_0/T)^\gamma + 1$ and $(\rho_m - \rho)/\rho_c \simeq (\rho_c - \rho_m)/\rho_c = N_4$ with $N_4 \simeq 0.07$ as predicted in [22]. Hence we get

$$\Lambda_{max} = \xi \delta N_4^\mu \left(\frac{T_0}{T}\right)^{\gamma(1+\frac{1}{\beta})} = \Delta^{\frac{1}{\beta}} \frac{k_B}{e} \left(\frac{T_0}{T}\right)^{\gamma(1+\frac{1}{\beta})} \tag{13}$$

where the second equality is obtained by using the Böttger *et al.* prediction $\Delta = (N_4^\mu \delta e \xi / k_B)^\beta$ [22]. Using Eq. (15), we can compare Λ_{max} to the blob length $\mathcal{L}_p = \xi (T_0/T)^{\gamma(1+\nu)}$ [14] :

$$\frac{\Lambda_{max}}{\mathcal{L}_p} = \frac{\Delta^{\frac{1}{\beta}} k_B}{e\xi} \left(\frac{T_0}{T}\right)^{\gamma(\frac{1}{\beta}-\nu)} \simeq \frac{\Delta^{\frac{1}{\beta}} k_B}{e\xi} \tag{14}$$

where the second equality comes from the fact that in our case, due to the experimental value of β, Λ_{max} *and* $\mathcal{L}_p$ *have critical exponents very close to each other* since $1/\beta - \nu$ is in the (-0.08, 0.07) interval. We thus find that $\Lambda_{max}(T)/\mathcal{L}_p(T)$ *does not depend on the temperature.* By inserting $k_B/(e\xi) = A/\Gamma$ in Eq. (15), we find $\Lambda_{max}(T)/\mathcal{L}_p(T) = A\Delta^{\frac{1}{\beta}}/\Gamma = (0.70 \pm 0.07)A$, using our fit result $\Delta^{\frac{1}{\beta}}/\Gamma = 0.70 \pm 0.07$. Hence, $\Lambda_{max}(T)/\mathcal{L}_p(T)$ *is not much smaller than* 1 which is the highest possible theoretical value. We thus conclude that in our sample the importance of the returns is strong.

This importance of the returns must also play a role on the onset of the non linear behavior which occurs at a field $F_{lim}(T)$. Indeed, according to Böttger *et al.* $F_{lim}/T = k_B/e\Lambda_{max}$ [22]. According to Pollak *et al.*, $F_{lim}/T = k_B/er_m$ with $r_m = (\xi/2)(T_0/T)^\gamma$ the hopping length. In our case, this latter prediction amounts to $F_{lim}/T \geq 1000\,\mathrm{V\,K\,m^{-1}}$ for $T \geq 500\,\mathrm{mK}$ (for lower temperatures we cannot go to $F \to 0$ because of too low currents). We clearly see on Figs. 7 and 8 that the non linear fit obtained above extends down to $F/T \simeq 150\,\mathrm{V\ K^{-1}\ m^{-1}}$. This is one order of magnitude smaller than the Pollak *et al.* prediction and in quite good agreement with the Böttger et al. result. We thus conclude that the F_{lim} behavior we find is consistent with the above derived results on the importance of returns.

VI. CONCLUSION

Our study of the electric field effects in variable-range hopping transport for amorphous $Y_{0.19}Si_{0.81}$ below 2 K exhibits several important features. First, we find that the length L characterizing the intermediate field regime has the order of magnitude and T dependence ($\simeq T^{-\gamma}$, with $\gamma = 1/2$) which is expected in the VRH models of Hill [13] or Pollak and Riess [9] stating that $L \simeq r_m$. Even analyzing our data in the framework of the Böttger, Bryksin *et al.* predictions (Eq. (3)) this result remains true, as the addition of the $B(eF\xi/(k_BT))^\beta$ term in Eq. (3) does not change the order of magnitude of this characteristic length. Second, our most important result is that Eq. (3) is much more relevant than Eq. (4) to analyze our data, and *this shows the importance of the "returns" in the percolation paths of VRH.* Furthermore, we were able to extract an information on the length of these returns from our experimental results. Indeed, our data indicate that the critical exponent of the returns contribution $1/\beta$ is very close to the one of the blob length : the returns represent an appreciable T-independent fraction of the whole percolation paths lengths at intermediate fields. Third, our very high field data do not follow the expected activationless law given by Eq. (2). This could be due to the onset of tunneling across the mobility edge whose interplay with activationless hopping has not been theoretically studied yet.

ACKNOWLEDGEMENTS

We want to thank J.P. Bouchaud, J.L. Pichard and M. Sanquer for fruitful discussions. Many thanks also to Y. Imry for explaining us Ref. [62].

APPENDIX A: IRRELEVANCE OF THE SAMPLE OR CARRIERS HEATING MECHANISM

In this Appendix, we first describe the experimental setup allowing thermal conductances measurements and then show that heating is irrelevant to account for our *I-V* non linearities.

The sapphire substrate was hold between four sapphire balls which represent a negligible thermal conductance. The thermalization was realised by ultrasonically bonding 43 gold wires (50 μm in diameter, a few millimeters long) between the cryostat ("Heat sink" on Fig. 1) and a 7 mm^2 gold pad schematized on the left of the substrate on Fig. 1. The resulting calculated thermal resistance between the gold pad and the cryostat is smaller than 10^4 K/W at $T = 50$ mK and 10^3 K/W at $T = 500$ mK, leading to a temperature difference lower than 0.5 mK between those two points in our experiments. To measure the thermal resistance between the cryostat and the sapphire substrate or the sample, we used the 1 MΩ heating resistor chip shown on the right up corner of Fig. 1. This 0.01 mm^3 device is held *only* by two Al wires (25 μm in diameter, 5 mm long) which are superconducting below $\simeq$ 1 K. At low temperature, their thermal conductance is thus negligible and the electrical power dissipated in the resistor flows to the substrate through the unique gold wire (25 μm in diameter, 3 mm long) ultrasonically bonded between the resistor and the gold pad evaporated on the sapphire substrate (on the right in Fig. 1). By measuring the temperature of the sample when a given power is injected in the resistor, this system gives an over-estimation of the thermal resistance between the sapphire substrate and the cryostat. It has the advantage of being reversible in comparison with a resistor deposited on the sapphire substrate, as the gold wire can be easily removed.

We show now that heating phenomena are irrelevant to account for the *I-V* non linearities. We first focus on the possible heating of the whole sample together with its sapphire substrate, and then turn to "electronic heating".

A. Heating of the whole sample and substrate

The measurement of the thermal resistance $\mathcal{R}_{th}$ between the cryostat on one hand and the sample with the sapphire substrate on the other hand was carried out as follows. A constant voltage $V = Fl$ was applied to the Y_xSi_{1-x} sample, leading to a current $I(F,T)$ depending on the cryostat temperature T. A given electrical power 1 nW $\leq \mathcal{P} \leq$ 100 nW was then dissipated in the small 1 MΩ resistor. This power flowed to the heat sink through the substrate whose temperature was then increased by δT, leading to an increase δI of the current. We checked that δI was proportional to $\mathcal{P}$. Assuming for a while that the *I-V* non linearities do not result from sample heating, we extracted, from the data of Fig. 2, δT from δI and deduced $\mathcal{R}_{th} = \delta T/\mathcal{P}$. Fig. 9 gives the resulting $\mathcal{R}_{th}$ as a function of T. From it, we get $\mathcal{R}_{th}(74\,\text{mK}) \simeq 10$ mK/nW, while we can see on Fig. 2 that the $I(F, 74\,\text{mK})$ and $I(F, 124\,\text{mK})$ curves begin to merge for $IV \simeq 0.04$ nW which corresponds to $\delta T \simeq 0.4$ mK much lower than the 50 mK separating these two $I(F)$ characteristics. This confirms the above assumption of irrelevance of sample heating; and it can be easily shown to be true at any temperature. Let us note that $\mathcal{R}_{th}$ exhibits a $\mathcal{R}_{th} \sim T^{-3}$ behavior which characterizes the Kapitza thermal resistance at the boundary between two materials. In our case, they are the sapphire substrate and the gold pad thermally connected to the cryostat.

B. Electronic heating

In this section, we show that the non-linearities of our *I-V* curves cannot be ascribed to a heating effect as found by Wang *et al.* for NTD sensors [44]. Assuming the validity of such a model for our sample, the power $P = IV = IFl$ injected in the YSi "electron bath" would increase its temperature to a value T_e larger than the cryostat temperature T, leading to a YSi electrical resistance

$$R(T,F) = R_0 \exp\left((T_0/T_e)^\gamma\right), \tag{A1}$$

with T_e given by

$$P + P_p = IV = g(T_e^\eta - T^\eta) \tag{A2}$$

where g and η are parameters characterizing the thermal conductance between the electron bath and the cryostat, and P_p is the parasitic power injected in the sample due to the limited rf shielding etc. As we have excluded a possible heating effect of the sapphire substrate (see previous section), the thermal resistance to consider is either the Kapitza one at the boundary between the YSi sample and the sapphire, or the thermal resistance due to electron-phonon coupling in the YSi itself. In the first case $\eta = 4$[63], while in the second one, $\eta = 5$ to 6 [44][47]-[53][64]. We investigated the experimental values of dP/dT_e, which would be equal to $g\eta T_e^{\eta-1}$, hence would not depend on T and P_p. Within the heating model, T_e can be extracted for each (I, V) point using Eq. (A1). Fig. 10 shows dP/dT_e as a function of T_e. The fact that most of the curves depend on T is a strong argument against the heating model. However, we can see a trend towards a T independence for low T values. As indicated by the straight lines corresponding to power laws, these low T curves are not compatible with the heating model because they correspond to η values which depend on T_e and may be much larger than 4 to 6. Finally, we note that in materials close to a-YSi, the electron-phonon coupling parameter g was found experimentally to be of the order of 10^3 W K^{-6}cm^{-3} (in NbSi, with $\eta = 6$) [52] or 200 W K^{-5}cm^{-3} (in AuGe, with $\eta = 5$) [64]. As a consequence, for our 7.2×10^{-5} cm^3 sample, we expect $dP/dT_e \simeq 0.4\,\mathrm{T}_e^5$ W/K or $dP/dT_e \simeq 0.07\,T_e^4$ W/K which is several orders of magnitude larger than what we find (see Fig. 10). If we assume that the possible heating effect is due to the YSi-sapphire Kapitza resistance, we can use the experimental $g \simeq (1-10) \times 10^{-3}$ W K^{-3}cm^{-2} values for sapphire-metal interfaces[51], which lead to dP/dT_e values of the order of $10^{-3}\,T_e^3$ W/K, again several orders of magnitude larger than our experimental values. Yet, those very large discrepancies guarantee that the heating effects are negligible. In comparison to data from authors who see heating effects, this can be explained by : i) our very resistive sample, ii) the low electron-phonon and Kapitza resistances due to the geometry of the sample.

APPENDIX B: ESTIMATION OF ξ AND ϵ_r FROM T_0 AND Γ.

The detailed calculations of A, B, α, $\alpha\prime$ and β were performed by Böttger *et al.* assuming Mott VRH ($\gamma = 1/(d+1)$) while we have $\gamma = 1/2$. Thus our fit result $A\xi = 1.1$ nm cannot be used straightforwardly to get ξ. In this appendix, we first try to estimate in which interval A must lie in the case of $\gamma = 1/2$ and then we use the value of T_0 as an additional experimental constraint on ξ.

It appears that the exponents α, α' and β should remain unchanged when going from $\gamma = 1/(d+1)$ to $\gamma = 1/2$. This can be readily seen for $\alpha = \alpha' = 1$ in the framework of Pollak's calculations [9]. Moreover, the fact that $\alpha = 1$ for $\gamma = 1/2$ is confirmed by many analyses of experimental results using Eq. (4) [29] [31] [35] [38] [40] [41] [42] [45]; while, in what concerns $\alpha\prime$ the experimental situation is unclear (see Sec. I). However, the prefactors A and B are likely to be changed by the presence of a Coulomb gap. In this case, we can state at least $A \leq 1/2$, since $A = 1/2$ comes from the replacement of $E_m/(k_BT) \simeq \frac{1}{2}(T_0/T)^\gamma$ by $E_m/(k_BT) - eFr_m/(k_BT)$ in Eq. (1). Such a substitution obviously overestimates I in the presence of an electric field since it neglects both the influence of returns and the insensitivity of a large number of pair currents with respect to F. From $A \leq 1/2$ we deduce $\xi \geq 2.2$ nm. Using the Böttger, Bryksin *et al.* value [22] [17] [18] $A = 1/6$, we find $\xi = 6.6$ nm which, using Eq. (5) gives $\epsilon_r = 29$, while $\xi \geq 2.2$ nm leads to $\epsilon_r \leq 86$.

According to Imry *et al.* [62], one expects $\epsilon_r = N_1(\xi/\lambda_{T.F.})^2$ where $\lambda_{T.F.}$ is the Thomas Fermi screening length and $N_1 = 1$ according to Abrahams and Lee [65]. Thus, using Eq. (5), $\lambda_{T.F.} \simeq 0.08A^{-3/2}$ nm which leads to $\lambda_{T.F.} = 1.2$ nm for $A = 1/6$ and $\lambda_{T.F.} \geq 0.23$ nm for $A \leq 1/2$. In crystalline metals with a concentration n of one electron per atom we have typically $\lambda_{T.F.} \simeq 0.06$ nm. Here we expect n to be of the order of 0.1 and since the standard screening theory yields $\lambda_{T.F.} \propto n^{-1/6}$, the value of 0.23 nm for our sample is plausible. However, we cannot exclude that the upper value of 1.2 nm is plausible too. Indeed, it was theoretically found [66] that close to the transition, electronic diffusion is considerably lowered, which should reflect in a lowering of screening, i.e. in an (unknown) increase of $\lambda_{T.F.}$. Moreover, if as recently suggested [67], many body effects come into play in Efros-Shklovskii VRH, one expect both a reduction of the 2.9 factor in Eq. (5) and a change of the A value. Finally, considering all these unknown effects, $A\xi$ is found to have the correct order of magnitude and we estimate that $\xi \approx 7$ nm.

The determination of the dielectric constant ϵ_r of the system is a very interesting working direction for the future due to the fundamental interest of ϵ_r in localization and MIT studies. This is also a strong argument in favor of a precise theoretical determination of the numerical parameters in Eq. (3). Even if those parameters are not completely known, the *relative* evolutions of ϵ_r as a function of the dopant concentration, magnetic field, etc. should be reachable with the ϵ_r extraction method we used.

* Electronic address : ladieu@drecam.cea.fr , Phone : (33) (0)169088558, Fax: (33) (0)169086923
† Electronic address : lhote@amoco.saclay.cea.fr , Phone : (33) (0)169083015

References

[1] P.W. Anderson, Phys. Rev. **109**, 1492 (1958).

[2] N.F. Mott, Phil.Mag. **19**, 835 (1969).

[3] V. Ambegaokar, B.I. Halperin, J.S. Langer, Phys. Rev. B **4**, 2612 (1971).

[4] M. Pollak, J. Non Cryst. Sol. **11**, 1 (1972).

[5] B.I. Shklovskii and A.L. Efros, *Electronic properties of doped Semiconductors*, Springer series in Solid-State Science Vol. 45 (Springer, New-York, 1984)

[6] A. Aharony, Y. Zhang, P. Sarachik, Phys. Rev. Lett. **68**, 3900 (1992).

[7] B.I. Shklovskii, Sov. Phys. Semicond. **6**, 1964 (1973).

[8] N. Apsley and H.P. Hughes, Phil. Mag. **30**, 963 (1974); N. Apsley and H.P. Hughes, Phil. Mag. **31**, 1327 (1975).

[9] M. Pollak and I. Riess, J. Phys. C **9**, 2339 (1976).

[10] B. I. Shklovskii, Sov. Phys. Semicond. **10**, 855 (1976).

[11] R. Rentzsch, I. S. Shlimak and H. Berger, Phys. Stat. Sol. (a) **54**, 487 (1979).

[12] M. Van Der Meer, R. Schuchardt, R. Keiper, Phys. Stat. Sol. B **110**, 571 (1982).

[13] R.M. Hill, Phil. Mag. **24**, 1307 (1971).

[14] B.I. Shklovskii, A.L. Efros, Usp. Fiz. Nauk. **117**, 401 (1975).

[15] S. Feng, J.L. Pichard, Phys. Rev. Lett. **67**, 753 (1991) and references therein.

[16] H. Böttger and V.V. Bryksin, Phil. Mag. B **42**, No 2, 297 (1980); H. Böttger and V.V. Bryksin, Phys. Stat. Sol. B **96**, 219 (1979).

[17] H. Böttger, P. Szyler, D. Wegener, Phys. Stat. Sol. B **128**, K179 (1985).

[18] H. Böttger, P. Szyler, D. Wegener, Phys. Stat. Sol. B **133**, K143 (1986).

[19] J. Talamantes, M. Pollak, R. Baron, J. Non Cryst. Sol. **97-98**, 555 (1987).

[20] E. I. Levin and B. I. Shklovskii, Sov. Phys. Semicond. **18**, 534 (1984).

[21] H. Böttger and V.V. Bryksin, Phys. Stat. Sol. B **113**, 9 (1982).

[22] H. Böttger and D. Wegener, Phys. Stat. Sol. B **121**, 413 (1984); H. Böttger and V.V. Bryksin in *Hopping Conduction in Solids*, pp. 236-259, VCH Publishers (USA), ISBN 0-89573-481-8; H. Böttger and D. Wegener, in *Hopping and Related Phenomena*, p. 317, H. Fritzsche, M. Pollak eds., World Scientific Publishing Company, (1990).

[23] J. Talamantes and J. Floratos, Phil. Mag. B **65**, No 4, 627 (1992).

[24] T.R. Kirkpatrick, Phys. Rev. B **33**, 780, (1986).

[25] We have $E_F = E_{Mob} - k_B T_1$ (see Sec. III) with the mobility edge E_{Mob} given by the Ioffe-Regel criterion $(2mE_{Mob})^{1/2}\lambda_{el} = \hbar$ where λ_{el} is the elastic mean free path. Since our sample is amorphous, $\lambda_{el} \simeq 0.3$ nm) yielding $E_{Mob} \simeq 0.35\,\mathrm{eV} \simeq E_F$. With $\xi = 2 - 6\,\mathrm{nm}$ (see Sec. V) it is found that $eF\xi \leq 10^{-4} \times E_F$ even for the maximum field used $4 \times 10^4\,\mathrm{V/m}$.

[26] M. Morgan and P. A. Walley, Phil. Mag. **27**, 1151 (1971).

[27] M. Telnic, L. Vescan, N. Croitoru and C. Popescu, Phys. Stat. Sol. (b) **59**, 699 (1973).

[28] J.M. Marshall and G.R. Miller, Phil. Mag. **27**, 1151 (1972).

[29] P.J. Elliott, A.D. Yoffe and E.A. Davis, American Institute of Physics Conf. Proc. **20**, 311 (1974).

[30] K. Nair and S.S. Mitra, J. Non-Crystalline Solids **24**, 1 (1977).

[31] A. N. Aleshin and I. S. Shlimak, Sov. Phys. Semicond. **21**, 289 (1987).

[32] A. V. Dvurechenskii, V. A. Dravin and A. I. Yakimov, JETP Lett. **48**, 156 (1988).

[33] C. E. Nebel, R. A. Street, N. M. Johnson and C. C. Tsai, Phys. Rev. B **46**, 6803 (1992).

[34] B. Popescu, T. Wright, C. J. Adkins and S. Iovan, Phys. Stat. Sol. B **205**, 77 (1998).

[35] D. Redfield, Adv. Phys. **24**, 463 (1975).

[36] A.G. Zabrodskii and I.S. Shlimak, Sov. Phys. Semicond. **11**, 430 (1980).

[37] T. F. Rosenbaum, K. Andres and G. A. Thomas, Solid State Comm. **35**, 663 (1980).

[38] A. N. Ionov, M. N. Matveev, I. S. Shlimak and R. Rentch, JETP Lett. **45**, 311 (1987).

[39] D. I. Aladashvili, Z. A. Adamiya, K. G. Lavdovskii, E. I. Levin and B. I. Shklovskii, in *Hopping and Related Phenomena*, edited by H. Fritzsche and M. Pollak (1990) pp. 283-297, World Scientific Publishing Company, (1990).

[40] T. W. Kenny, P. L. Richards, I. S. Park, E. E. Haller and J. W. Beeman, Phys. Rev. **39**, 8476 (1989).

[41] Chen Gang, H. D. Koppen, R. W. van der Heijden, A. T. A. M. de Waele and H. M. Gijsman, Solid State Comm. **72**, 173 (1989).

[42] I. N. Timchenko, V. A. Kasiyan, D. D. Nedeoglo and A. V. Simashkevich, Sov. Phys. Semicond. **23**, 148 (1989).

[43] F. Tremblay, M. Pepper, R. Newbury, D. Ritchie, D. C. Peacock, J. E. F. Frost and G. A. C. Jones, Phys. Rev. B **40**, 3387 (1989).

[44] N. Wang, F.C. Wellstood, B. Sadoulet, E. E. Haller and J. Beeman, Phys. Rev. B **41**, 3761 (1990).

[45] S. M. Grannan, A. E. Lange, E. E. Haller, J. W. Beeman, Phys. Rev. B **45**, 4516 (1992).

[46] R. W. Van der Heijden, G. Chen, A. T. A. M. de Waele, H. M. Gijsman and F. P. B. Tielen, Phil. Mag. B **65**, 849 (1992).

[47] P. Stephanyi, C. C. Zammit, P. Fozooni, M. J. Lea and G. Ensell, J. Phys.: Condens. Matter **9**, 881 (1997).

[48] A. Alessandrello *et al.*, in *Proceedings of the 5th Int. Workshop on Low Temperature Detectors*, edited by S. E. Labov and B. A. Young (Berkeley, July 29 - August 3 1993), J. Low Temperature Physics **93** (3/4) (1993) pp. 207-212 and pp. 337-342; M. Frank *et al. ibid.*, pp. 213-218; E. Aubourg *et al. ibid.*, pp. 289-294; L. Dumoulin *et al. ibid.*, pp. 301-306; N. Perrin *et al. ibid.*, pp. 313-317; J. Soudee *et al. ibid.*, pp. 319-324; K. Djotni *et al. ibid.*, pp. 325- 329; X. X. Wang *et al. ibid.*, pp. 349-354.

[49] A. Alessandrello *et al.*, in *Proceedings of the 6th Int. Workshop on Low Temperature Detectors*, edited by H.R. Ott and A. Zehnder (Beatenberg, Switzerland 28 August - 1 September 1995), Nucl. Inst. and Meth. **A** 370 (1995), pp. 244 - 246.

[50] A. Alessandrello *et al.*, in *Proceedings of the 7th Int. Workshop on Low Temperature Detectors*, edited by S. Cooper (Munich, 27 July - 2 August 1997) pp. 138-141; S. M. Grannan and P. L. Richards *ibid.*, pp. 160-161.

[51] D. Yvon, L. Bergé, L. Dumoulin, P. De Marcillac, S. Marnieros, P. Pari, G. Chardin, Nucl. Inst. and Meth. A **370**, 201 (1996).

[52] L. Dumoulin, L. Bergé, S. Marnieros, J. Lesueur, Nucl. Inst. and Meth. A **370**, 211 (1996).

[53] N. Perrin, J. Appl. Phys. **82**, 3341 (1997).

[54] M. Sanquer, R. Tourbot, B. Boucher, Europhys. Lett. **7**, 635 (1988).

[55] J.L. Pichard, M. Sanquer, K. Slevin, P. Debray, Phys. Rev. Lett. **65**, 1812 (1990).

[56] P. Hernandez and M. Sanquer, Phys. Rev. Lett. **68**, 1402 (1992).

[57] P. Hernandez, F. Ladieu, M. Sanquer, D. Mailly, Physica B **194-196**, 1141 (1994).

[58] M. Specht, L.P. Levy, F. Ladieu, M. Sanquer, Phys. Rev. Lett. **75**, 3902 (1995).

[59] F. Ladieu, M. Sanquer, J.P. Bouchaud, Phys. Rev. B **53**, No 3, 973 (1996).

[60] S.M. Sze, *Physics of Semiconductor Devices*, (Wiley, New York, 1981), p. 403.

[61] The choice of Ψ was also motivated by the fact that we first tried to analyze our $I(F,T)$ dependence by using $\Phi(F,T) = \sqrt{(T/T_0)}\ln\left[(I(F,T) - I_{E.S.})/I_1\right]$, expanding on the intuition that the current $I(F,T)$ might be the *sum* of the linear current $I_{E.S.}(F,T)$ deduced from Eq. (1) and of a non linear current given by Eq. (3). This failed since Φ appears to *be negative* at low F/T, and particularly $\Phi(F \to 0, T) \ll 0$. Very importantly, when $F/T \geq 3 \times 10^4$ V K^{-1}m^{-1}, I_1 can be chosen such that $\Phi(F,T) \simeq \Psi(F,T)$. The values of α, β, A, B obtained from a fit of Ψ are thus consistent with those from a fit of $\Phi(F/T)$ for $F/T \geq 3 \times 10^4$V K^{-1}m^{-1}.

[62] Y. Imry, Y. Gefen, D.J. Bergman, Phys. Rev. B **26**, 3436 (1982).

[63] E.T. Schwartz and R.O. Pohl, Rev. Mod. Phys. **61**, 605 (1989).

[64] J. R. Cooper, W. P. Beyermann, S. W. Cheong and G. Gruner, Phys. Rev. B **36**, 7748 (1987).

[65] E. Abrahams, P.A. Lee, Phys. Rev. B **33**, 683, (1986).

[66] E.P. Nakhmedov, V.N. Prigodin, Y.A. Firtov, Sov. JETP **65**, 1202, (1987); P. Sebbah, D. Sornette, C. Vanneste, Phys. Rev. B **48**, 12506 (1993).

[67] A. Prez-Garrido, M. Ortuno, E. Cuevas, J. Ruiz, M. Pollak, Phys. Rev. B **55**, R8630 (1997); J. Talamantes and A. Moebius, Phys. Stat. Sol. B **205**, 45 (1998).

Figure Captions

FIG. 1. Experimental setup: the $9\,\mu$m thick $Y_{0.19}Si_{0.81}$ layer is deposited onto a sapphire substrate with two interdigited gold electrodes. Thermalization of the sample was ensured by 43 gold wires (4 represented) bonded on the left gold pad. Upper right corner : small $1\,\mathrm{M}\Omega$ chip heater allowing thermal resistance measurements at low temperature (see Appendix A).

FIG. 2. Current as a function of electric field at various temperatures below 1.3 K : for clarity only 18 out of the 36 different curves were represented. Inset: $R(F \to 0)$ vs. $1/T$ (dots), for temperatures above 4 K. The dashed line corresponds to an activated law with a characteristic temperature of 40 K.

FIG. 3. Logarithm of the resistance as a function the electric field to temperature ratio, for 14 temperatures among the 28 measured ones.

FIG. 4. Normalized value of $T^{-\gamma}$ for 3 values of γ as a function of the logarithm of the resistance at zero electric field. The normalized $T^{-\gamma}$ is $(T^{-\gamma} - T_{Min}^{-\gamma})/(T_{Max}^{-\gamma} - T_{Min}^{-\gamma})$ where T_{Min} and T_{Max} are the two extreme values of the temperature T selected for the plot. Inset : residue (i.e. measured minus fitted value) of the linear fit of $\ln[R(F \to 0)]$ as a function of $T^{-\gamma}$, for $\gamma = 1/4$ (open circles) and $\gamma = 1/4$ (closed circles).

FIG. 5. Effective exponent of the current vs electric field law, as a function of the electric field, for 6 temperatures.

FIG. 6. The length L extracted from the slopes of the $\ln(V/I)$ vs F/T lines at $F \to 0$ using Eq. (4) (dots), and the fitted $L = L_0\ (T_0/T)^{1/2}$ law (continuous line).

FIG. 7. The $\Psi(F,T)$ function (given by $(T/T_0)^{1/2} \ln(I/I_{E.S.})$, with $I_{E.S.} = (V/R_0)\exp[-(T_0/T)^{1/2}]$) as a function of F/T for all the data except the very high field points. Ψ increases more slowly than F/T (the dashed line corresponds to $\Psi \propto F/T$) and its evolution can be fitted (solid line) using the Böttger *et al.* prediction $\Psi = \Gamma(F/T) - \Delta(F/T)^{\beta}$ with $\beta = 1.15 \pm 0.1$, $\Gamma = (1.25 \pm 0.5) \times 10^{-5}\ \mathrm{K\,m\,V^{-1}}$ and $\Delta^{1/\beta}/\Gamma = 0.70 \pm 0.07$. Inset : same Ψ vs. F/T dependence with linear scales showing that the $\Delta(F/T)^{\beta}$ term plays a role at low F/T values; the dashed line corresponding to $\Psi \propto F/T$.

FIG. 8. F/T dependence of $\Gamma(F/T) - \Psi(F,T)$, with $\Gamma = 1.25 \times 10^{-5}\mathrm{K\,m\,V^{-1}}$, for all the data points except the very high field ones. The dashed line corresponds to a $\Delta(F/T)^{\beta}$ dependence with $\beta = 1$, and shows that $\beta > 1$. Solid line : fit with $\beta = 1.15$ and $\Delta = 1.4 \times 10^{-6}(\mathrm{Km/V})^{\beta}$. Inset : same data with linear scales, the dashed line corresponding to a $\sim F/T$ dependence.

FIG. 9. Thermal resistance $\mathcal{R}_{th}(T)$ measured by dissipating a controlled power in the small $1\,\mathrm{M}\Omega$ chip (see Fig. 1). Dashed line : fit of the data with a T^{-3} law.

FIG. 10. Derivative of the power dissipated in the YSi sample with respect to the effective electron temperature T_e, as a function of T_e. For each (I,V) point, T_e is calculated using Eq. (A1). The points line up in curves corresponding to different cryostat temperatures among which 5 are indicated in the figure. For comparison, the three straight lines correspond to 3 power laws $dP/dT_e \propto T_e^{(\gamma-1)}$ with $\gamma - 1 = 3$, 5 and 9.

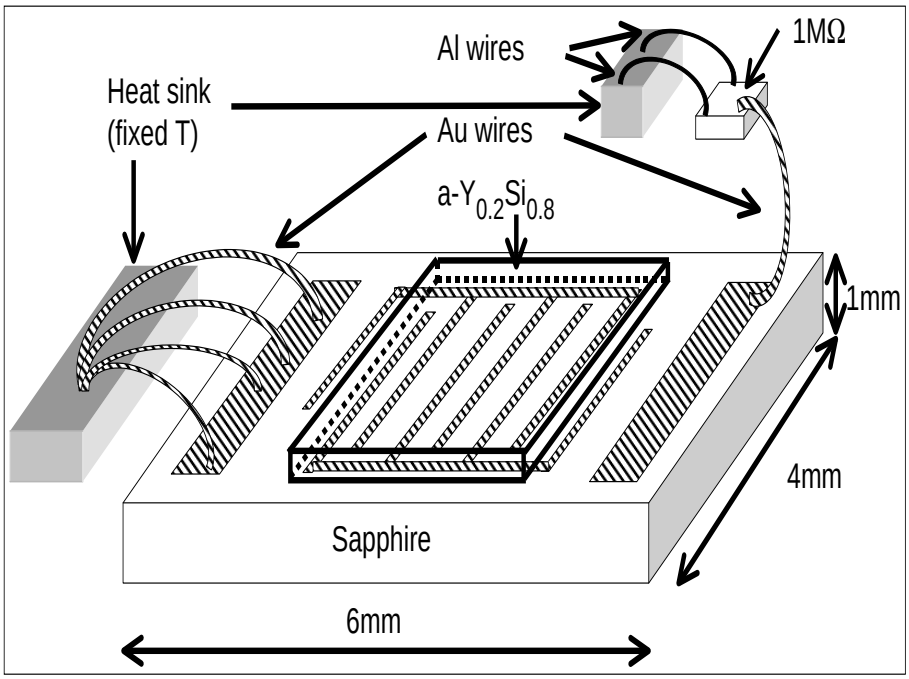
Al wires
1MΩ
Heat sink
(fixed T)
Au wires
a-Y0.2Si0.8
1mm
4mm
Sapphire
6mm

Figure 1

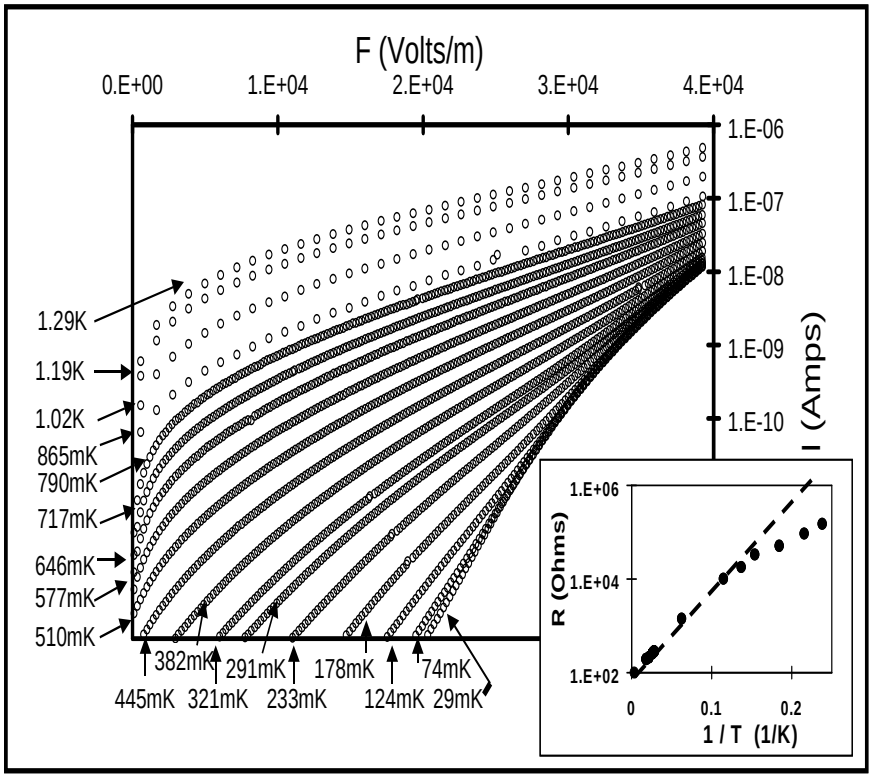
F (Volts/m)
0.E+00
1.E+04
2.E+04
3.E+04
4.E+04
1.E-06
1.E-07
1.E-08
1.E-09
1.E-10
I (Amps)
1.29K
1.19K
1.02K
865mK
790mK
717mK
646mK
577mK
510mK
445mK
382mK
321mK
291mK
233mK
178mK
124mK
74mK
29mK
1.E+06
1.E+04
1.E+02
R (Ohms)
0
0.1
0.2
1 / T (1/K)

Figure 2

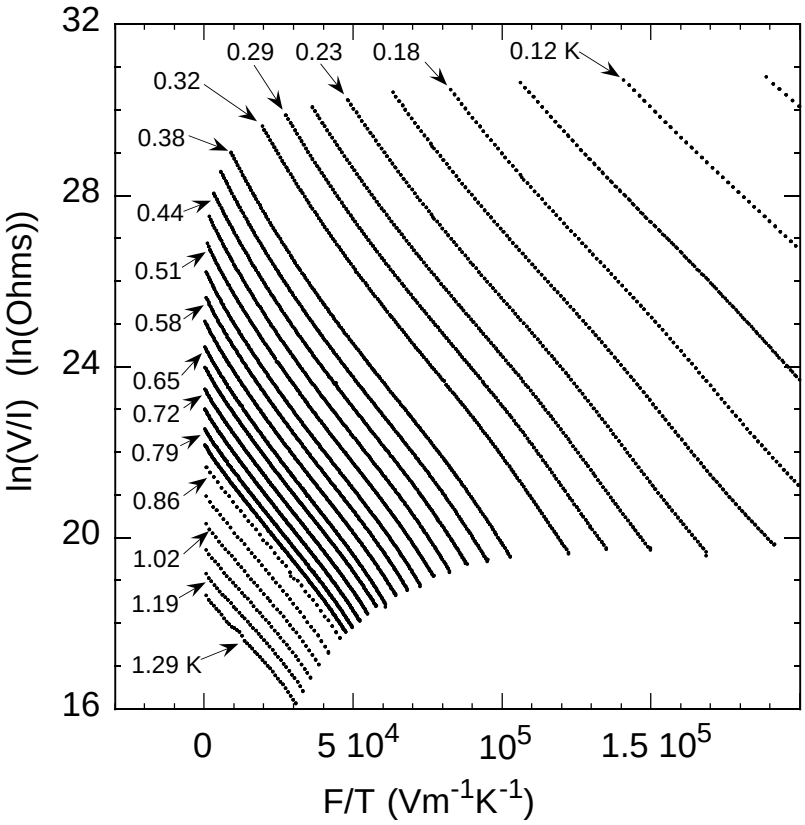
32
28
24
20
16
ln(V/I) (ln(Ohms))
0
5 10^4
10^5
1.5 10^5
F/T (Vm^-1K^-1)
0.12 K
0.18
0.23
0.29
0.32
0.38
0.44
0.51
0.58
0.65
0.72
0.79
0.86
1.02
1.19
1.29 K

Figure 3

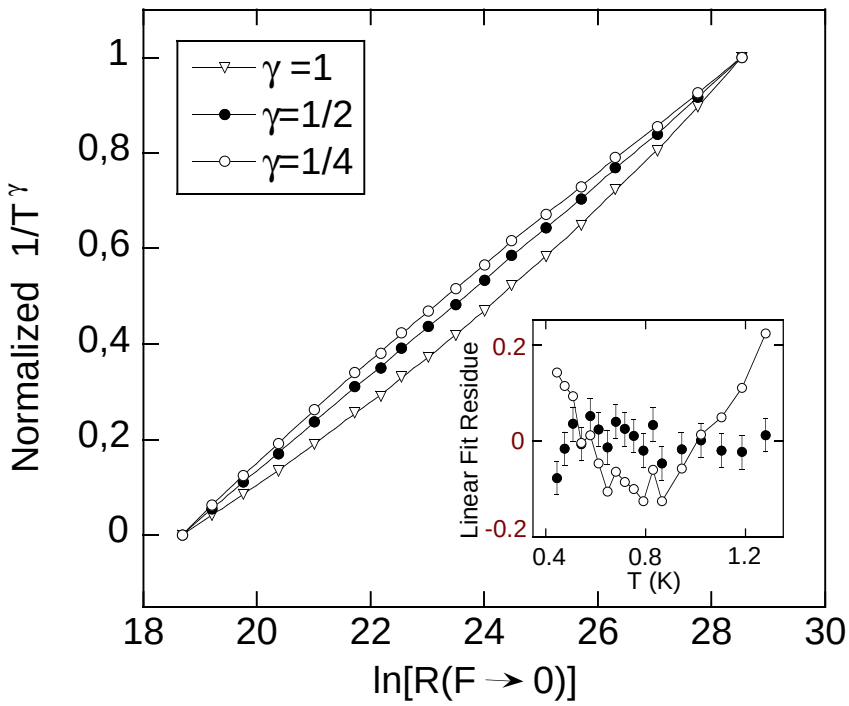

Figure 4

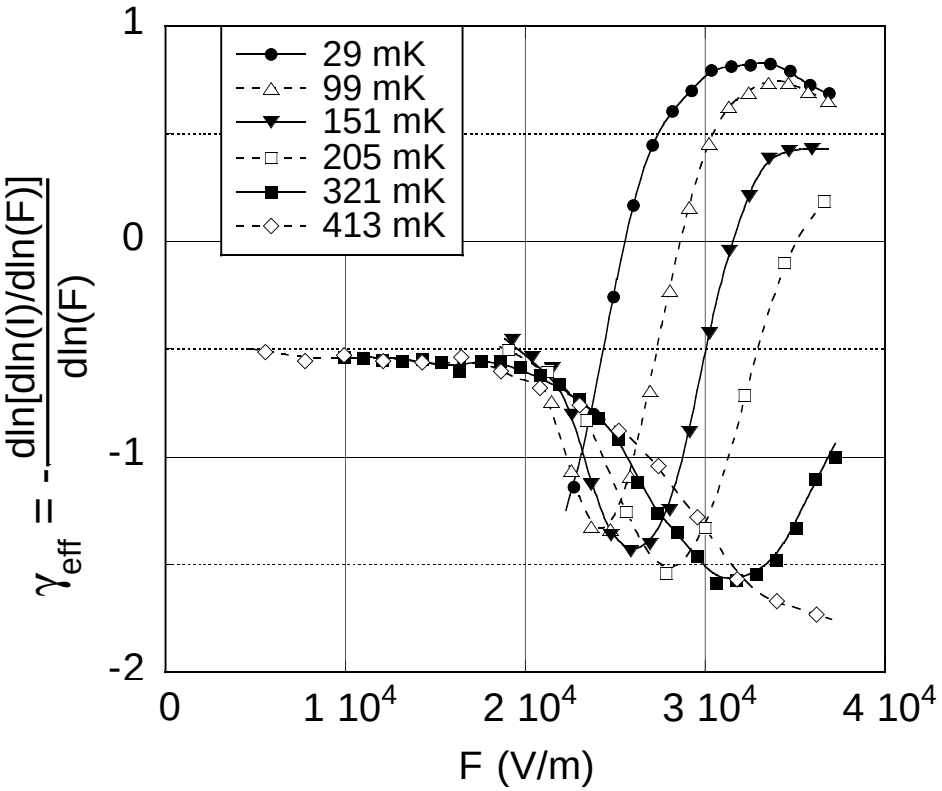
1
0
-1
-2
0
1 10^4
2 10^4
3 10^4
4 10^4
F (V/m)
29 mK
99 mK
151 mK
205 mK
321 mK
413 mK
γeff = - dln[dln(I)/dln(F)] / dln(F)

Figure 5

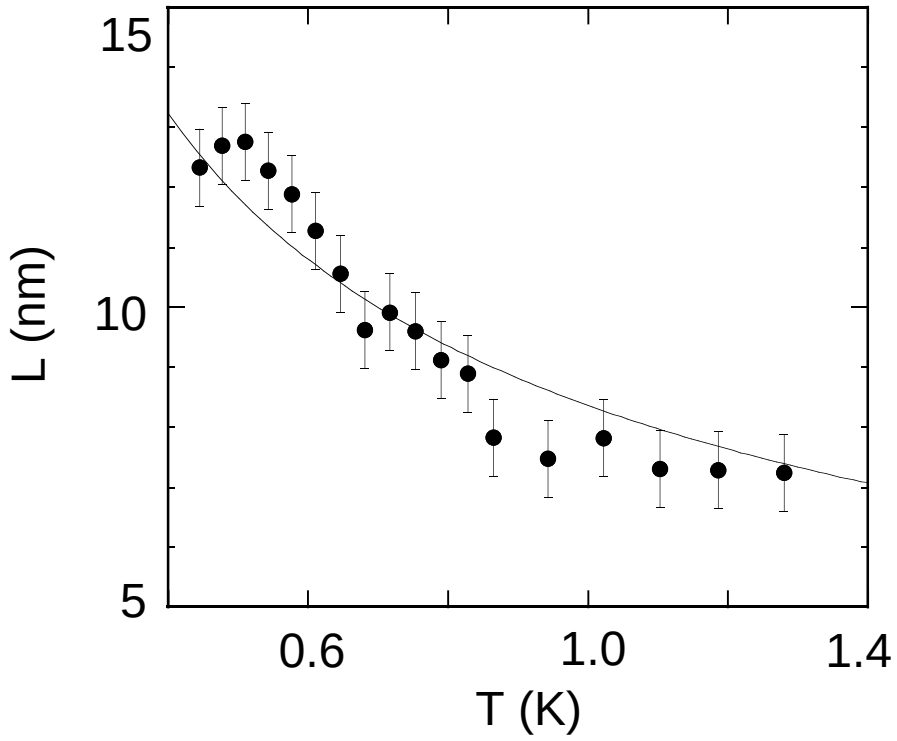

Figure 6

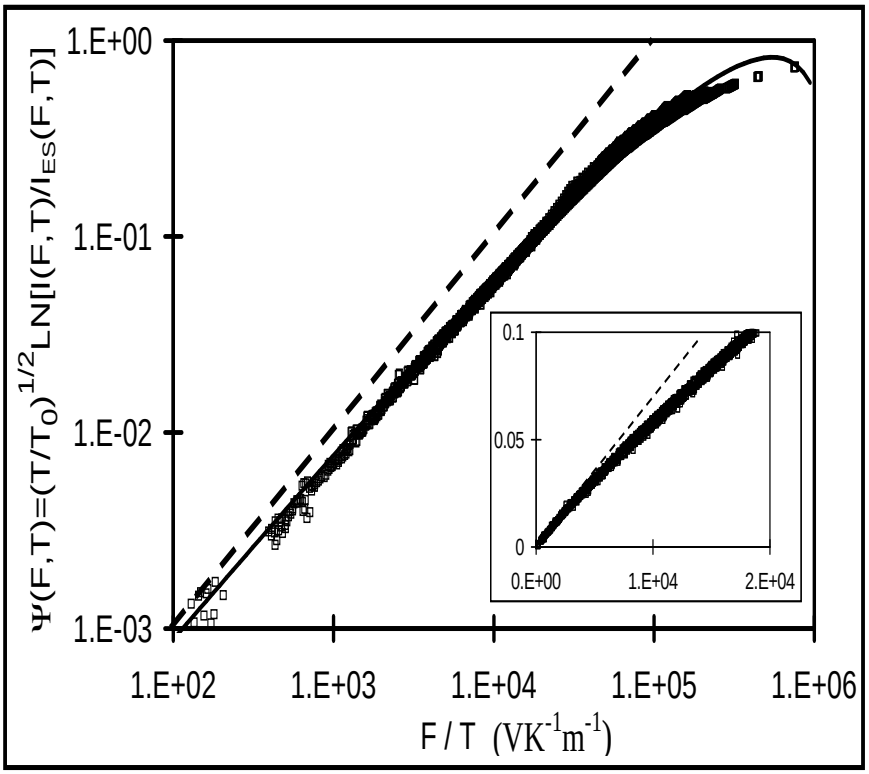
1.E+00
1.E-01
1.E-02
1.E-03
Ψ(F,T)=(T/T_O)^1/2 LN[I(F,T)/I_ES(F,T)]
1.E+02
1.E+03
1.E+04
1.E+05
1.E+06
F / T (VK^-1m^-1)
0.1
0.05
0
0.E+00
1.E+04
2.E+04

Figure 7

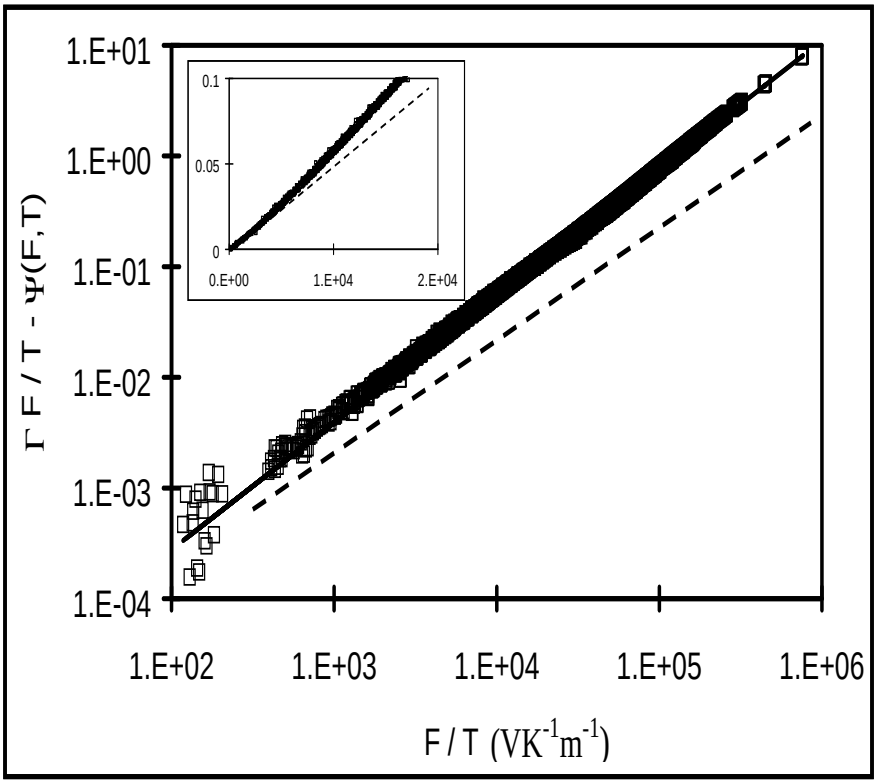
1.E+01
1.E+00
1.E-01
1.E-02
1.E-03
1.E-04
Γ F / T - Ψ(F, T)
1.E+02
1.E+03
1.E+04
1.E+05
1.E+06
F / T (VK-1m-1)
0.1
0.05
0
0.E+00
1.E+04
2.E+04

Figure 8

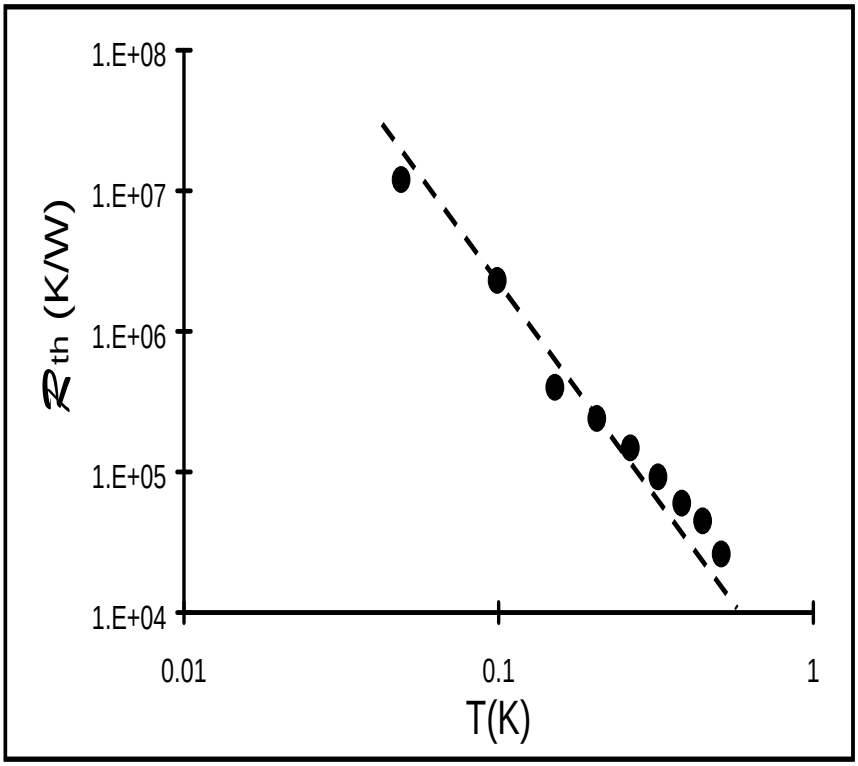

Figure 9

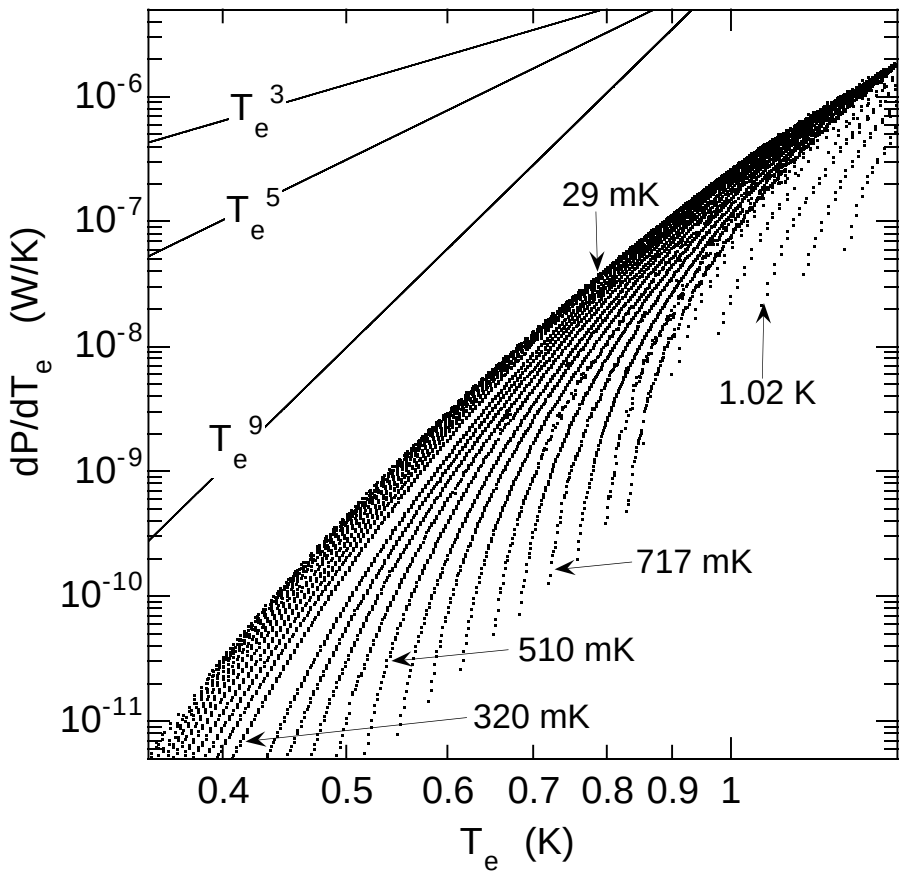
10^{-6}
10^{-7}
10^{-8}
10^{-9}
10^{-10}
10^{-11}
dP/dT_e (W/K)
T_e^3
T_e^5
T_e^9
29 mK
1.02 K
717 mK
510 mK
320 mK
0.4
0.5
0.6
0.7
0.8
0.9
1
T_e (K)

Figure 10